Impurity density determination using charge exchange and beam emission spectroscopy at ASDEX Upgrade

R. Dux, B. Geiger, R. M. McDermott, L. Menchero[1], T. Pütterich, E. Viezzer
and ASDEX Upgrade team

Max-Planck-Institut für Plasmaphysik, EURATOM Association, Garching, Germany.
[1] *University of Strathclyde, Glasgow, United Kingdom.*

The determination of impurity density profiles from charge exchange recombination spectroscopy (CXRS) on the neutral heating beam is performed by analysing the *active* impurity emission, which is induced by charge exchange reactions between beam neutrals and impurity ions. To this end, the densities of the three neutral beam species with full, half and third energy are required and are usually just calculated from models for the beam geometry (position, direction and profile), for the fraction of each species to the total beam power and for the attenuation of each component in the plasma. Lately, the beam observation optics of one toroidal CXRS system at ASDEX Upgrade has been refurbished and equipped with 3 rows of 30 fibres. This offered the possibility to simultaneously measure CXRS and the D_α emission of the beam. The D_α beam emission is proportional to the population of beam atoms excited to the n=3-level and can be used to cross-check the neutral beam density evaluation. Due to the different Doppler shift of the three energy components, the beam emission spectroscopy (BES) delivers information on all energy components. A forth D_α component is due to thermal beam halo neutrals, which are produced by charge-exchange(CX) from beam neutrals to plasma deuterons. It turned out that these halo neutrals produce a considerable fraction of the *active* impurity emission.

Experimental Setup

In a H-mode plasma (#26333) with constant NBI heating power of 5 MW and ECRH power of 0.7 MW at medium density of $6\times10^{19} \text{m}^{-3}$, the analysis method has been tested for CXRS measurements of boron using the n=7-6 transition of B^{4+} at λ=494.5 nm. Each of the four 60 keV-beams of the NBI-1 box is intersected by the lines-of-sight (LOS) and was individually switched on for 200 ms and off for 100 ms to allow for good separation of the beam emission from the background radiation. During the periods without injection from NBI-1 the missing power was replaced by a beam from the second NBI system. Only the more tangential beams 2 and 3 provide sufficiently large Doppler shift of the D_α-lines, especially for the plasma edge, such that the three energy components can be separated in the spectra. Fig.1 shows a cross-section of the relative neutral density of these beams. The co-ordinate l shows along the beam into the plasma and v along the beam height. The coloured areas give the density relative to the centre in 10% steps. The symbols denote the position where the LOS are closest to the beams (crosses for BES, stars for CXRS). Obviously, the LOS are designed for measurements on beam 3, while beam 2 moves out of the observed region when approaching the plasma centre.

Fig.1: *Position of the closest approach of LOS and beams (crosses for BES, stars for CXRS) and beam density cross-section.*

The fitting of the beam emission spectra with its line-splitting due to the motional Stark effect is quite involved and has previously been explained [1]. We just want to point out that the D_α radiances of all beam components $L_{\alpha,j}$ and of the halo neutrals L_α^h of all LOS are fitted simultaneously to all measured spectra at one time point. To this end,
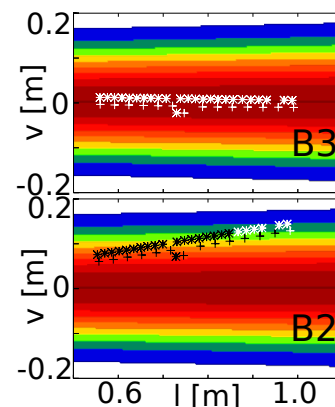
the radiances are parametrized with a cubic-spline function along the beam, which are then multiplied with an individual geometrical factor for each LOS that represents the LOS integral of the non-attenuated beam density for that LOS. For the presented results, a spline with 4 knots was used. Thus, the fit-result can easily be transformed from the BES-LOS onto the CXRS-LOS by just exchanging the individual geometrical factors. Considering the typical LOS separation of $\Delta Z \approx 1.6$ cm between BES and CXRS and the typical $1/e$-width of the beam of 12 cm the ratio of these geometrical factors is close to 1 for beam 3 and just important for beam 2. The halo cloud has a somewhat wider extent than the beams and the ratio of these geometrical factors is then even closer to 1. Therefore, the exact knowledge of the shape of the halo cloud, which is not known during the fit, is not so important. We assumed a 30% larger decay length perpendicular to the beam, which turned out to be justified by the later analysis.

Fig.2 shows in the top row the obtained D_α radiance profiles for the CXRS-LOS versus the average poloidal flux-label ρ_{pol} of the LOS within the beam. On the left, the results for beam 3 are depicted and radiances from beam 2 are on the right. The radiation from the full energy beam component is shown in black (E1), red is used for second (E2) and blue for third energy (E3). For beam 2, the decay is stronger due to the misalignment of beam and LOS. One of the LOS is outside the row of the other LOS, which leads to an extra increase of L_α for beam 2 and nearly no change for beam 3 at this LOS. The halo (H) shown in cyan produces the largest radiances. Fig.3 displays in the top row the measured radiance profiles for the boron transition at $\lambda = 494.5$ nm (green,m) and gives in the second row the profiles of the electron density n_e and the electron and ion temperature, T_e and T_i, which were taken for the further analysis.

Fig.2: *Profiles for beam emission and derived quantities versus ρ_{pol} measured during #26333. left column: beam 3, right column: beam 2. top row: measured radiances of the D_α radiation from halo neutral (H,cyan) and beam neutrals of the first (E1,black), second (E2,red) and third (E3,blue) energy component. middle row: line-of-sight integrals of the neutral density from above measurements and form beam attenuation calculation. bottom row: change of line-of-sight integral g_h due to the wider halo cloud.*

Evaluation of Boron Densities

The D_α emission is proportional to the population of atoms excited to the $n=3$-level, which can be calculated with collisional-radiative (CR) models. To this end, A-values for radiative decay and cross-section formulas for excitation, de-excitation, ionisation and charge transfer due to collisions with electrons, deuterium ions and impurities have been collected from the literature [2, 3] in order to calculate the appropriate rate coefficients for beam-thermal or thermal-thermal reactions and to set-up CR models up to the $n=10$-level for the beam and halo neutrals respectively. The CR models are used to get equilibrated excited state populations of the beam, effective beam stopping rates and state resolved halo neutral creation rates and also the excited state population and loss rates for the halo neutrals. For the beam, the CR model can also be solved time dependently following the beam neutrals as they penetrate the plasma. However, even for the 60 keV neutrals and at $n_e = 6 \times 10^{19}$m^{-3}, it only takes about 2 cm until the fractional
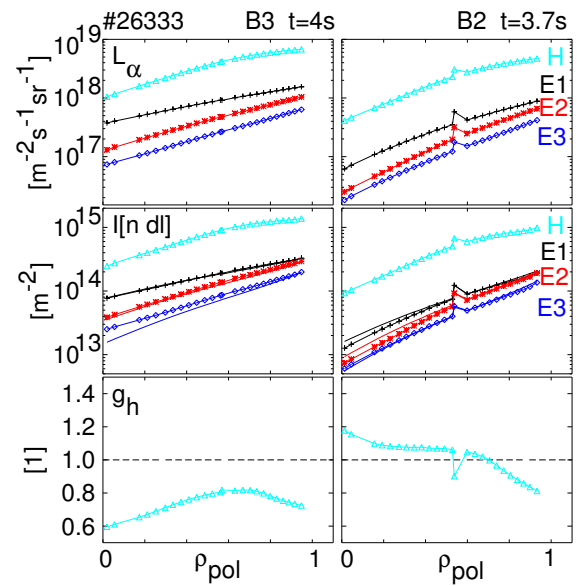
population of the n=3-level deviates less than 10% from the equilibrium value. Thus, only the outermost LOS, which is about 2-3 cm inside the steep gradient region of the H-mode barrier, might see a non-equilibrated excited state population of the beam.

The D_α radiance for beam component j is:

$$L_{\alpha,j} = n_e q_{\alpha,j} \int_{los} n_{b,j} dl, \qquad (1)$$

where $q_{\alpha,j}$ is an effective photon emission co-efficient (PEC) depending on the beam energy and all plasma parameters. The plasma parameters shall be mean values for the LOS volume inside the beam. The state population of the halo neutrals is influenced by the source distribution, with which they were born which in turn differs for the three beam energies. Thus, the PEC $q_{\alpha,j}^h$ is different for each part of the halo density $n_{h,j}$ depending on the parent beam energy and the radiance is a sum of three terms:

$$L_\alpha^h = n_e \sum_j q_{\alpha,j}^h \int_{los} n_{h,j} dl. \qquad (2)$$

This is a complication, since we have only one measurement of L_α^h and three unknowns. However, the CR model also delivers the ratio r_j of halo neutrals to beam neutrals and the LOS integral of the individual halo density component is:

$$\int_{los} n_{h,j} dl = g_h\, r_j \int_{los} n_{b,j} dl \qquad (3)$$

Fig.3: *Profiles for imputity emission and derived quantities measured during #26333. left: beam 3, right: beam 2. top row: measured radiance of the boron n =7-6 transition (m, green) and calculated contributions from halo and beam neutrals. second row: n_e, T_e, and T_i. third row: CX photons per D_α photon for c_B=1. bottom: derived boron concentration with and without considering the halo neutrals.*

where g_h is a geometric factor due to the wider extent of the halo cloud compared with the beam. Thus, the fraction $f_j = \int_{los} n_{h,j} dl / \int_{los} n_h dl$ of halo component j to the total halo density can easily be derived. For the active CX-emission of an impurity with concentration c_{imp}, we get a similar expression.

$$L_{cx} = n_e c_{imp} \sum_j \left[q_{cx,j} \int_{los} n_{b,j} dl + q_{cx,j}^h \int_{los} n_{h,j} dl \right] = c_{imp} \left[\sum_j L_{\alpha,j} \frac{q_{cx,j}}{q_{\alpha,j}} + L_\alpha^h \frac{\sum_j f_j q_{cx,j}^h}{\sum_j f_j q_{\alpha,j}^h} \right] \qquad (4)$$

The effective PEC $q_{cx,j}$ for energy component j includes the charge exchange from ground state and excited state beam atoms and also depends on the above plasma parameters. For the effective PEC $q_{cx,j}^h$ from halo neutrals, mainly excited state halo atoms are important for the ion temperature range in ASDEX Upgrade. The PEC's were calculated with ADAS routines [3]. Thus, the impurity concentration can be calculated from the measured radiances for the impurity charge exchange line and the Balmer radiations. The various factors q_{cx}/q_α denote the number of CX-photons per D_α photon for an impurity concentration of 1. For the halo component, this factor is replaced by a weighted average of the respective q_{cx} and q_α values.

The second row of fig.2 depicts the LOS integrals of the densities as calculated from the measured radiances. The profiles look quite similar to the L_α profiles since for the given plasma parameter, the PEC's are only weak functions of the radius. The beam density integrals can also be compared with the result of a beam attenuation calculation, drawn with solid lines of the same colour. In this calculation we replaced the nominal power fractions of the beam species
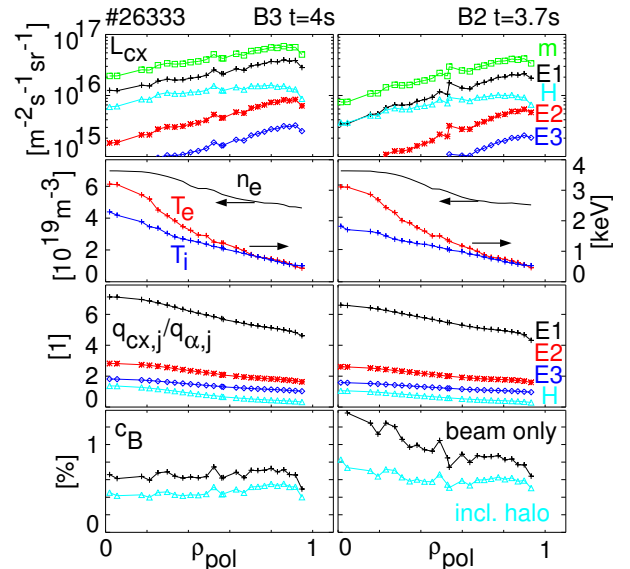
$f_{p,j}$=0.66, 0.26, 0.08 by the values which fit the beam emission ratios at the outermost LOS: 0.67, 0.23, 0.10 for beam 3 and 0.66, 0.24, 0.10 for beam 2. For the beam species, which contribute most to the CX radiation of boron, the agreement is better than 5% for beam 3, while for beam 2, it deviates up to 20% in the centre. The bottom row of fig.2 shows g_h being below 1 for the chords which centrally intersect the beam and above 1 when seeing only the periphery of the beam. These values agree with a factor 1.2-1.4 larger halo compared to the beam and do also prove that the calculated ratios of halo to beam neutrals r_j are consistent with the measurement.

The third row of fig. 3 displays the number of CX-photons per D_α photon at c_B=1. Here, the values are lowest for the halo neutrals. However, the contribution of the halo to the total CX-radiance is large due to the large number of halo neutrals as can be seen in the top row of fig.3. For beam 2, it equals the E1 contribution in the centre of the plasma since here g_h is above 1. Thus, it is important to include the halo into the derivation of the boron concentration as can be seen in the bottom graphs of fig. 3, where especially for the cen-

Fig.4: *Ratio of halo to beam induced CX-lines as a function of beam energy and plasma temperature.*

tre channels at beam 2 the influence is large. For beam 3, the proper CX-beam, the changes are up to 50%, but the profile shape is almost unchanged.
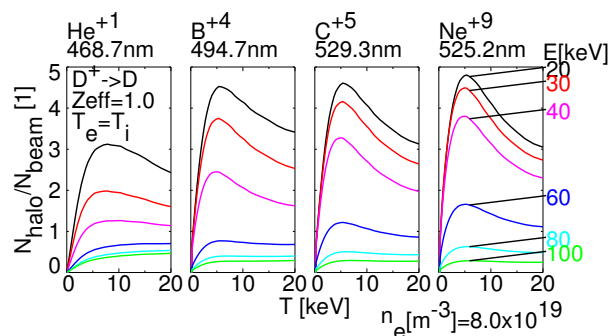
Conclusion

A test of the application of BES to the determination of impurity densities showed, that the atomic data for calculation of the excited state population are sufficiently good to get extra information on the beam attenuation from the measured radiance profiles of D_α. A combined treatment of BES data and beam attenuation calculations will be the optimum solution for future analysis tools, since the uncertainties of the beam attenuation are very low in the edge while BES can improve the uncertainty in the centre. A proper assessment of the uncertainties has still to be done. One systematic effect, that so far has been thought to be only important at very high T_i values of 20-30 keV [4], is the CX excited impurity radiation from halo neutrals. Even at low values of T_i, the effect is quite strong due to charge transfer from excited deuterium in the n=2 level. Fig. 4 gives an overview for popular visible lines from He, B, C and Ne. The lines at different colours show the ratio of emitted photons N_{halo} due to CX from halo compared to CX from beam neutrals N_{beam} for various deuterium beam energies versus the temperature of a deuterium plasma (T_i=T_e). This ratio reflects the ratio of the respective line integrals along the LOS for g_h=1. The effect is strongest for low beam energies since halo production by charge transfer to deuterium is highest. The halo to beam density ratio peaks around 3-4 keV, while the effective CX is always rising with temperature shifting the local maximum to larger temperatures. At high temperatures, charge transfer from ground state halo neutrals sets in. This happens first for the lighter impurities.

References

[1] R. Dux et al, Proceedings 38th EPS Conf. on Plasma Phys., Strasbourg (2011)P1.056.
[2] R.K. Janev et al, IAEA-APID-4 (1993).
[3] H.P. Summers, ADAS User Manual 2.6 (2004). http://www.adas.ac.uk./manual.php
[4] B.C. Stratton et al, Nucl. Fusion **30**(1990)675.